

## Preparation and Characterization of Sodium Poly( $\alpha$ ,L-glutamate)/Poly(ethylene oxide) Macromolecular Complexes

Kariyawasam P. Pemawansa, Alka Thakur, Emmanuel K. Karikari, and Ishrat M. Khan\*

Department of Chemistry, Clark Atlanta University, Atlanta, Georgia 30314

Received November 10, 1998

**ABSTRACT:** Two series of macromolecular complexes of poly(ethylene oxide) (PEO) [100K and 600K]/sodium poly( $\alpha$ ,L-glutamate) (PGNA) [MW 1K and 45K] and poly(ethylene glycol) [MW 350–2000]/PGNA [1K] have been prepared by solution blending using water/methanol mixtures. All the macromolecular complexes were soluble in water. The PGNA/PEO macromolecular complexes were mechanically reliable opaque films and may be stretched a couple of fold to form white opaque fibrils. Formation of the  $\alpha$ -helical conformation of PGNA in the complexes was determined by CD studies; e.g., the CD spectrum of a film of PGNA 1K–PEO 600K (1:2.5, w/w) complex showed a positive peak at 200 nm and two negative peaks at 207 and 220 nm, indicating the presence of the  $\alpha$ -helical PGNA conformation in the complex. FT-IR spectra of the complexes support the presence of the  $\alpha$ -helical PGNA conformation in the macromolecular complexes. Wide-angle X-ray diffraction (WAXD) patterns of the PGNA 1K–PEO 600K (1:2.5 and 1:5, w/w) indicate that some of the PEO crystalline segments in the complex form a near planar zigzag conformation. Solution  $^{23}\text{Na}$  and 2D-NOESY  $^1\text{H}$  NMR spectra of the complexes in nonaqueous solvents revealed interaction between the PEO and PGNA at the following sites:  $\text{CH}_2\text{--CH}_2$  (of PEO) and  $\gamma\text{--CH}_2\text{--}$  (of PGNA) [hydrophobic interaction] and  $\text{O}^- \cdots \text{Na}^+$  [ion–dipole interaction]. In aqueous solutions, ion–dipole complex sites dissociated completely to form free (solvated) sodium ions, and the number of contact points interacting through hydrophobic interactions was reduced significantly and diminished in dilute solutions. The proposed solid-state structure of the macromolecular complex is a helical PGNA core; PEO crystalline segments having near planar zigzag conformations; glutamate and ethylene oxide segments interacting through ion–dipole interaction; and  $\beta$  and  $\gamma$  groups of PGNA side groups interacting with PEO segments through hydrophobic interactions.

### Introduction

Poly(ethylene oxide) (PEO) and its lower molecular weight analogue, poly(ethylene glycol) (PEG), are important biocompatible polymers. Because of the non-toxicity and nonantigenic activity of PEO and PEG, these polymers have important applications as colloid for stabilizing food and paints and as formulating agents in pharmaceuticals and cosmetics.<sup>1</sup> A number of other potential biotechnical applications of PEO and PEG are in protein-resistant coatings, immunosensors, control drug release, and targeted delivery of drugs.<sup>1–3</sup> Derivatives of PEG such as PEG block copolymers, e.g., biodegradable poly(lactic acid)-*b*-poly(ethylene glycol), have been generally utilized for prolonging the circulation half-lives of proteins or for delivering targeted payloads of protein pharmaceuticals to specific tissues with minimal toxicity.<sup>2–4</sup> Detailed studies on the preparation, structural characterization, and investigation of properties of such poly(ethylene glycol) block copolymers and the cross-linked hydrogel form of the block copolymers have been reported recently.<sup>2,5,6</sup> Poly(ethylene glycol) segments in the copolymers are known to stabilize or preserve the three-dimensional structure of the proteins and in some cases even induce helical structures to random chain polypeptide.<sup>5</sup>

Poly(ethylene oxide) is known to form aggregates with surfactants such as sodium dodecyl sulfate<sup>7</sup> and complexes with small molecules such as *p*-dihalogenobenzene, *p*-nitrophenol, and resorcinol.<sup>8–10</sup> Earlier work in our laboratory demonstrated that intimate blending of PEO and poly(2-vinylpyridine) (P2VP) took place only when an optimum amount of lithium ions was available.<sup>11,12</sup> Intimate blending of the two polymers resulted

from  $\text{N}^- \cdots \text{Li}^+ \cdots \text{O}^-$  ion–dipolar interactions linking PEO segments with P2VP segments. In this paper, we report on the formation of macromolecular complexes of PEO or PEG and sodium poly( $\alpha$ ,L-glutamate) (PGNA). Sodium poly( $\alpha$ ,L-glutamate) (PGNA) was selected as the initial model polypeptide because of the following reasons: (A) poly(glutamic acid) and PGNA are among the most thoroughly studied polypeptides;<sup>13</sup> (B) PGNA is also known to form stoichiometric complexes with oppositely charged surfactants to yield well organized three-dimensional microstructures;<sup>14</sup> (C) the high possibility of inducing helical conformations to low molecular weight (1000) PGNA by complex formation. Because of the formation of well-organized three-dimensional microstructure of certain PGNA–surfactant complexes, they have been identified as having potential applications in molecular composites, optoelectronics, and separation membranes.<sup>14–16</sup> These applications are also a possibility for well-organized three-dimensional macromolecular complexes of PEO or PEG/PGNA, and therefore, our goals are to determine the processing conditions that promote the formation of such microstructures in the PGNA–PEO system.

### Experimental Section

Poly(ethylene oxide) (PEO), poly(ethylene glycol) (MPEG and PEG), and PGNA supplied by Sigma Chemical Co. were used without further purification. Preparations of PGNA–MPEG complexes were carried out by solution mixing in methanol/water (80/20, v/v) mixtures, followed by evaporation of the solvent at reduced pressure over  $\text{P}_2\text{O}_5$ . The free MPEG was removed by extracting with benzene. The PEO/PGNA complexes were prepared by the same procedure using methanol/water mixtures. Films of the complexes and PEO [600K]

were solvent cast on glass plates or polystyrene dishes. The films were dried first at 40 °C under vacuum and finally for 24 h at 40 °C under vacuum over P<sub>2</sub>O<sub>5</sub>. Weak adhesion of the films to plastic dishes enabled removal of the films without stretching.

**Measurements.** Solution NMR spectra were acquired on a Bruker ARX 400 spectrometer at room temperature using D<sub>2</sub>O and CDCl<sub>3</sub> as solvents. TMS was used as the external standard for obtaining <sup>13</sup>C and <sup>1</sup>H spectra, and the standard for <sup>23</sup>Na spectra was a saturated NaCl solution.<sup>17,18</sup> Proton decoupled carbon spectra were recorded using single pulse acquisition at 45° pulse angle and 5 s relaxation delay for a 17 h acquisition period. <sup>23</sup>Na NMR spectra were recorded using single pulse acquisition at 10  $\mu$ s pulse width and 5 s relaxation delay for a given number of acquisitions.

The 2D-NOESY <sup>1</sup>H NMR analysis of the complexes were carried out using standard NOESY pulse sequence<sup>5,19</sup> under the following acquisition conditions:

*Experimental Condition I:* 4000 data points; relaxation delay, 50 ms; mixing time, 50 ms; number of scans, 8.

*Experimental Condition II:* 1024 data points; relaxation delay, 4.5 ms; mixing time, 20 ms; number of scans, 8.

Condition 1 has long relaxation and mixing times and more data points, allowing observation of even weak interactions, whereas in condition II, shorter mixing and relaxation times allow observation of the strong interactions place within a close proximity.

The glass transition temperature (*T*<sub>g</sub>) and melting temperature (*T*<sub>m</sub>) were determined by differential scanning calorimetry (DSC) using a Perkin-Elmer DSC-4 equipped with a thermal data station. Samples were scanned at a heating rate of 15 °C/min under N<sub>2</sub> to 100 °C and quenched cooled at a 320 °C/min to the starting temperature before obtaining the thermograms.

The circular dichroism (CD) spectra of thin films of the complexes were obtained using a JASCO 710 spectrophotometer at 20 nm/min speed and 0.5 nm resolution. Fourier transform infrared (FT-IR) spectra of the solid films were obtained using a Nicolet Impact 400 IR spectrophotometer. Transmission spectra were recorded by coadding 8 scans at 4 cm<sup>-1</sup> resolution at room temperature. Wide-angle X-ray diffraction (WAXD) studies of thin-film samples were conducted using a Philips X'pert MultiPurpose diffractometer. The thin-film sample stage, which consists of a collimated beam optical setup and a special Eulerian cradle, was used. The translations afforded by the Eulerian cradle permit a wide range of reflections from samples of any orientation to be studied. Diffraction data were collected with a PC-MRD software that has a user interface based on a reciprocal space model. The thin-film samples of the complexes and PEO 600K standard were irradiated with Cu K $\alpha$  X-rays (wavelength  $\lambda$  = 1.5406 Å) at a scan rate of 2°/min. Data were taken over a diffraction angle range of 10–50° (2 $\theta$ ), corresponding to *d* spacings of 8.8–1.8 Å.

## Results and Discussion

The solubility and physical characteristics of the PGNA (1K)/PEO or PEG macromolecular complexes are listed in Table 1. PGNA (1K)/MPEG (MW 350 and 550) or PEG (2K) macromolecular complexes are white powders and are soluble in water and water/methanol mixtures. The stoichiometry of the MPEG or PEG/PGNA complexes was determined using proton NMR peak area comparison, and therefore, in this instance a PGNA–MPEG (1:2.5) complex indicates a molar ratio of 1 mol of PGNA to 2.5 mol of MPEG. The stoichiometry of PGNA–PEO (*x*:*y*) complexes is based on the feed ratio, *x* grams of PGNA:*y* grams of PEO used in the preparation. Solution cast films of the PEG or MPEG based complexes had no mechanical strength and are not film forming. Most likely the molecular weights of MPEG and PEG are not sufficiently high for the

**Table 1. Solubility and Physical Characteristics of the Macromolecular Complexes<sup>a</sup>**

complex	solubility in		physical appearance
	H <sub>2</sub> O	benzene	
PGNA 1K–MPEG 350 and 550 (1:2.5)	S	NS	white powder
PGNA 1K–PEG 2000 (1:5)	S	S	white powder
PGNA 1K–PEO 100K (1:5)	S	partially <sup>b</sup>	hazy films
PGNA 1K–PEO 600K (1:5)	S	S	hazy films
PGNA 1K–PEO 600K (1:2.5)	S	NS	hazy films
PGNA 1K–PEO 600K (1:10)	S	NS	hazy films
PGNA 45K–PEG 2K (1:5)	S	NS	white powder
PGNA 45K–PEO 600K (1:5)	S	NS	hazy films

<sup>a</sup> S = soluble. Formed colorless clear transparent solutions at room temperature with occasional mixing within 1 h. NS = not soluble. Films remained in benzene at room temperature for > 48 h with occasional mixing. <sup>b</sup> Film lost its mass in benzene and reduced more than 50% of its thickness at room temperature within 1 h. The remaining thin film stayed in benzene for > 48 h with occasional mixing.

formation of a pseudo-cross-linked network due to ion–dipole interactions.<sup>11,12</sup> Complexes started to show good mechanical properties once the molecular weight of PEO surpasses 100K. Complexes prepared using high molecular weight PEO (600K) were mechanically strong and showed excellent adhesion to the substrate when prepared on glass and paper. Solution cast films of PGNA 1K–PEO 600K complexes peeled off from plastic dishes as hazy films and could be stretched to form white opaque fibrils. While every complex was soluble in water, benzene solubility of complexes appears to be dependent on the stoichiometry and the molecular weights of the components. A stoichiometry of 1:5 (PGNA–PEO) and PGNA molecular weight of 1K appear to be a prerequisite for benzene solubility. The PGNA 1K–PEO 600K (1:5) complex was completely soluble in benzene whereas both starting materials were insoluble in benzene. This indicates that because of the strong interaction between PGNA and PEO, the nature of the complex is sufficiently different from the individual components. The optimum complex stoichiometry of 1:5 required for benzene solubility may be understood in terms of the formation of an optimum number of glutamate–ethylene oxide interacting sites, leaving a minimum number of uncomplexed PGNA and PEO segments. The increase in molecular weight of PGNA leading to benzene-insoluble materials may be understood in terms of the increased ability to link two or more PEO chains by one PGNA, forming cross-linked type materials. The PGNA 1K–PEO 600K (1:5) complex was also soluble in other organic solvents such as chloroform. The observation of organic solubility is consistent with the solubility characteristics of other PGNA/surfactant complexes.<sup>14,20–23</sup>

Differential scanning calorimetry (DSC) thermograms of PGNA–MPEG complexes showed new glass transitions attributable to the formation of the complexes. For the PGNA–MPEG (350) and for the PGNA–MPEG (550) complexes new glass transition temperatures at –2 and 17 °C, respectively, were observed. The starting materials PGNA and the MPEGs do not have glass transition temperatures in this region. The amorphous phase of MPEG-350 should have a *T*<sub>g</sub> around –70 °C range, but ion–dipole interaction of the MPEG segments with the sodium ion of the polyglutamate decreases segmental motion and hence an increase in the *T*<sub>g</sub> is observed. Similar types of observations have been made in MPEG/alkali metal salt complexes prepared as

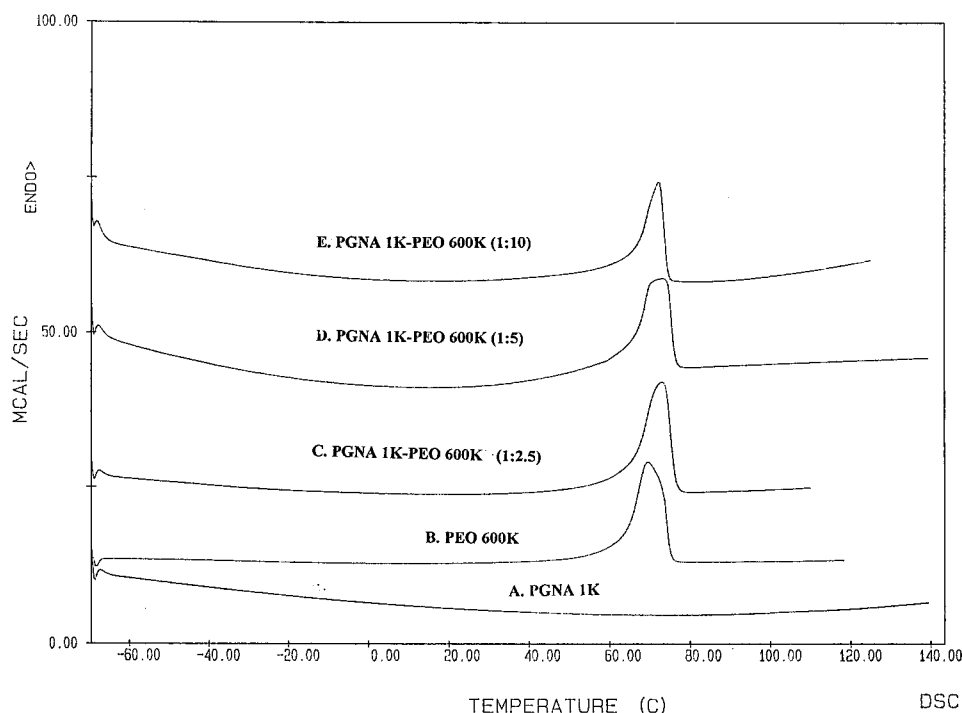


**Figure 1.** DSC thermograms of (A) PGNA 1K, (B) PEO 600K, (C) PGNA 1K-PEO 600K (1:2.5), (D) PGNA 1K-PEO 600K (1:5), and (E) PGNA 1K-PEO 600K (1:10).

solid polymer electrolytes.<sup>24</sup> The PGNA (1K)-PEO (600K) macromolecular complexes showed interesting thermal properties (Figure 1). The melting point of the complexes was somewhat higher than the melting point of pure PEO. The higher melting temperature of PEO crystalline phase may be attributed to the reorganization of some of the PEO chains in the PGNA-PEO macromolecular complexes. The ethylene oxide- $\text{Na}^+$  ion-dipolar interaction present in the complexes may induce this. The reorganization of the PEO chains is further supported by WAXD studies discussed in a following section.

The CD spectrum of PGNA-MPEG (1:2.5) showed a positive peak at 226 nm and two negative peaks at 204 and 230 nm indicative of an  $\alpha$ -helical PGNA conformation.<sup>25</sup> Since PGNA 1K is known to be in the random conformation even in the solid state,<sup>14,26-27</sup> the helical conformation of PGNA must have been induced by the complex formation. Helical conformation was much more pronounced in the solid films of the complexes prepared with higher molecular weight PEO. The CD spectrum of a film of the PGNA 1K-PEO 600K (1:2.5) complex (Figure 2A) showed a positive peak at 200 nm and two negative peaks at 207 and 220 nm, indicating formation of the  $\alpha$ -helical PGNA. The CD spectra of the PGNA-PEO (1:10) complex showed slightly different peak positions and shape compared to the CD of the 1:2.5 complex. This may be understood in terms of lower content of the PGNA in the 1:10 complex and a resulting reduction in the glutamate-ethylene oxide interactions and perhaps the induction of the  $\alpha$ -helical conformation of the PGNA is incomplete. FT-IR spectra of the complexes confirm the formation of an  $\alpha$ -helical structure by the polypeptide chain, as shown by the position of the amide I band at 1651, 1655, and 1648  $\text{cm}^{-1}$  for the PGNA 1K-PEO 600K complexes with stoichiometry of 1:2.5, 1:5, and 1:10, respectively. The position of the amide I band in these complexes is consistent with the amide I band observed at 1653  $\text{cm}^{-1}$  for the  $\alpha$ -helical

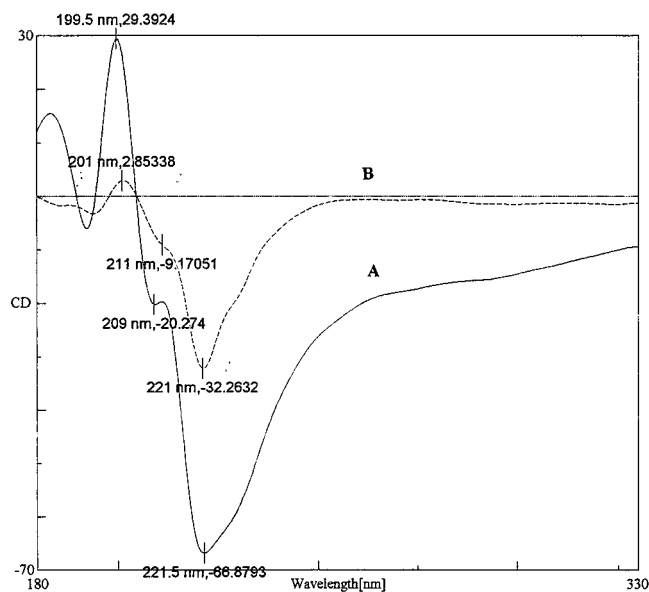


**Figure 2.** CD spectra of PGNA 1K-PEO 600K complex films having feed ratios: (A) 1:2.5; (B) 1:10.

PGNA conformation in PGNA-surfactant complexes.<sup>15</sup> The helical conformation of PGNA, most likely, permits increased ion-dipole interactions, resulting in the formation of the thermodynamically favorable and stable PGNA-PEO macromolecular complex; i.e., a PGNA helix with the glutamate groups on the outside would permit maximum interaction of the sodium ions with the ethylene oxide of the PEO chains. A nonhelical or random conformation may shield some sodium ions from interacting with the PEO chains.

A comparison of the WAXD of PGNA 1K-PEO 600K (1:2.5 and 1:5) complexes with that of pure PEO 600K showed (Figure 3 and Table 2) the following changes: (A) reduction in the intensity for the peak at 3.79 Å; (B) increase in the intensity for the peak at 4.61 Å; (C)



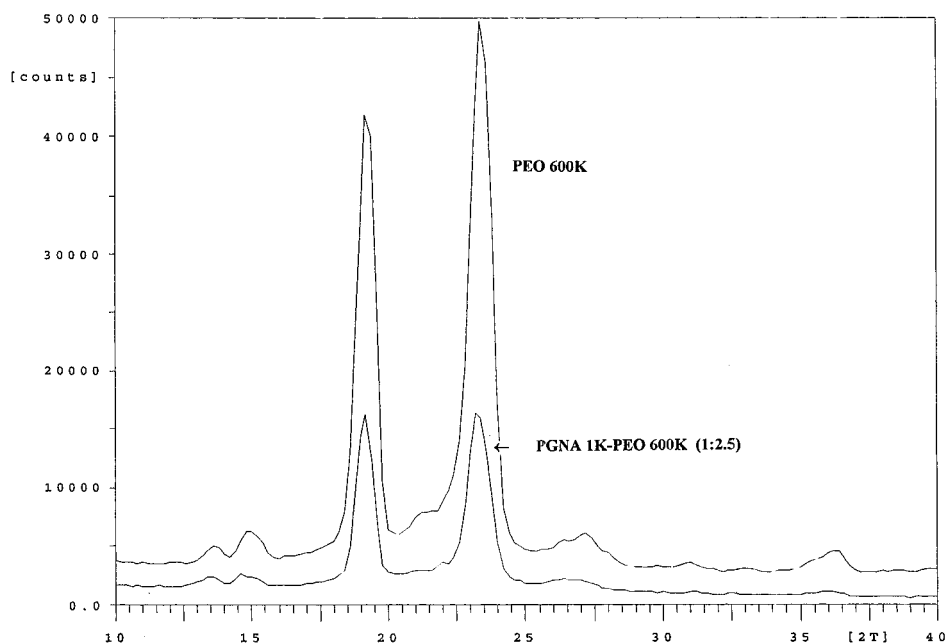


**Figure 3.** WAXD curves of PGNA 1K-PEO 600K (1:2.5) (bottom) and PEO 600K (top) films.

**Table 2. Relative Intensities and *d* Spacings of the Wide-Angle X-ray Diffraction Peaks of PEO 600K and PGNA 1K-PEO 600K (1:2.5 and 1:5) Complexes**

PGNA 1K-PEO 600K (1:2.5)		PGNA 1K-PEO 600K (1:5)		PEO 600K	
<i>d</i> spacing (Å)	rel int (%)	<i>d</i> spacing (Å)	rel int (%)	<i>d</i> spacing (Å)	rel int (%)
6.58	5.6	6.63	2.5	6.52	3.0
5.98	5.5	5.95	6.0	5.91	5.5
4.63	100	4.65	94.7	4.61	86.6
				4.19	4.9
3.81	97.3	3.80	100	3.79	100
3.28	2.5	3.30	4.1	3.27	3.5
2.87	0.7	2.90	1.7	2.88	1.1
		2.47	3.4		

slight increase in *d* spacing and increase in the intensity for the peak at 6.52 Å. Pure PEO has two prominent peaks at 4.61 and 3.79 Å with relative intensities 86.6% and 100%, respectively. These two *d* spacings can be assigned to the distance between PEO chains on *x*-*y* plane. Reduced intensity at 3.79 Å and increased intensity at 4.61 Å observed for the complexes may be attributed to a change in packing distance between PEO chains. Some of the chains having short packing distance, 3.79 Å, must have been enlarged to 4.61 Å by the complex formation with PGNA. The distance between monomer units along the PEO chain (*z*-axis) is known to be 3.56 Å for planar zigzag (stretched form) and 2.78 Å for 7/2 helical conformation (unstretched form).<sup>28</sup> However in PEO-HgCl<sub>2</sub> complexes, intermediate conformations (GTGGTG and T5GT5G) between planar zigzag and 7/2 helical conformation having *d* spacings 11.75 and 5.88 Å corresponding to the distance between monomer units along the PEO chain have been observed.<sup>29</sup> The observed *d* spacings 6.58 and 6.63 Å for the 1:2.5 and 1:5 complexes are slightly larger than the *d* spacing of the corresponding PEO peak at 6.58 Å. The observed *d* spacings of the complexes also fall between the corresponding *d* spacings for the distance between monomer units along the PEO chain for planar zigzag form ( $2 \times 3.56 \text{ Å} = 7.12 \text{ Å}$ ) and 7/2 helical conformation ( $2 \times 2.78 \text{ Å} = 5.56 \text{ Å}$ ). Observation of near planar zigzag PEO conformations in the complexes indicates that the

end-to-end distance of PEO segments are enlarged, and presumably PEO segments are stretched during formation of the complex. This complements the DSC data indicating the reorganization of some of the PEO crystalline chains in PEO/PGNA complexes. The structure of the complex in the solid state can be described as a composite consisting of PGNA helical core with PEO crystalline blocks that are anchored to the PGNA via sodium ion-dipole interaction (Figure 4A).

Molecular interactions in the macromolecular complexes were also monitored by NMR spectroscopy in different solvents under various conditions. Two-dimensional (2D) NOESY <sup>1</sup>H NMR spectra (Figure 5) of the PGNA 1K-PEO 600K (1:2.5) complex in D<sub>2</sub>O (about 50 mg/mL) obtained under experimental condition I showed strong correlation between PEO protons and  $\gamma$  protons of the PGNA, no correlation between amide NH protons of PGNA and PEO protons, weak correlation between  $\alpha$  protons of PGNA and PEO protons, and no correlation between  $\beta$  protons of PGNA and PEO protons. These observations suggest that the PEO and the PGNA are within close enough proximity to permit interactions. The observations are quite similar to the 2D-NOESY <sup>1</sup>H NMR results obtained using experimental condition II for a PEG block copolymer with poly(lysine) by Harada et al.<sup>5</sup> in which the methylene groups of the covalently linked PEG segment were in close proximity with the  $\epsilon$ -methylene groups of poly(L-lysine). Identical interactions in D<sub>2</sub>O solutions were also observed for the other complexes, PGNA 1K-PEO 600K (1:5) and PGNA 1K-PEG 2K (1:2.5 and 1:5), by 2D-NOESY <sup>1</sup>H NMR spectra under the same experimental conditions. In concentrated aqueous solutions, the structures of these complexes (Figure 4B) may be described as a composite with the following components: (A) helical or random chain PGNA; (B) random coil PEO chains; (C) some methylene groups of PEO chains within close proximity of  $\gamma$  protons of PGNA. Since methylene groups of PEO and  $\beta$  and  $\gamma$  groups of PGNA are hydrophobic, the nature of interaction in these complexes in D<sub>2</sub>O at the "PGNA  $\gamma$  protons-PEO methylene protons" site must be hydrophobic. The effect of dilution on molecular interactions of the complexes

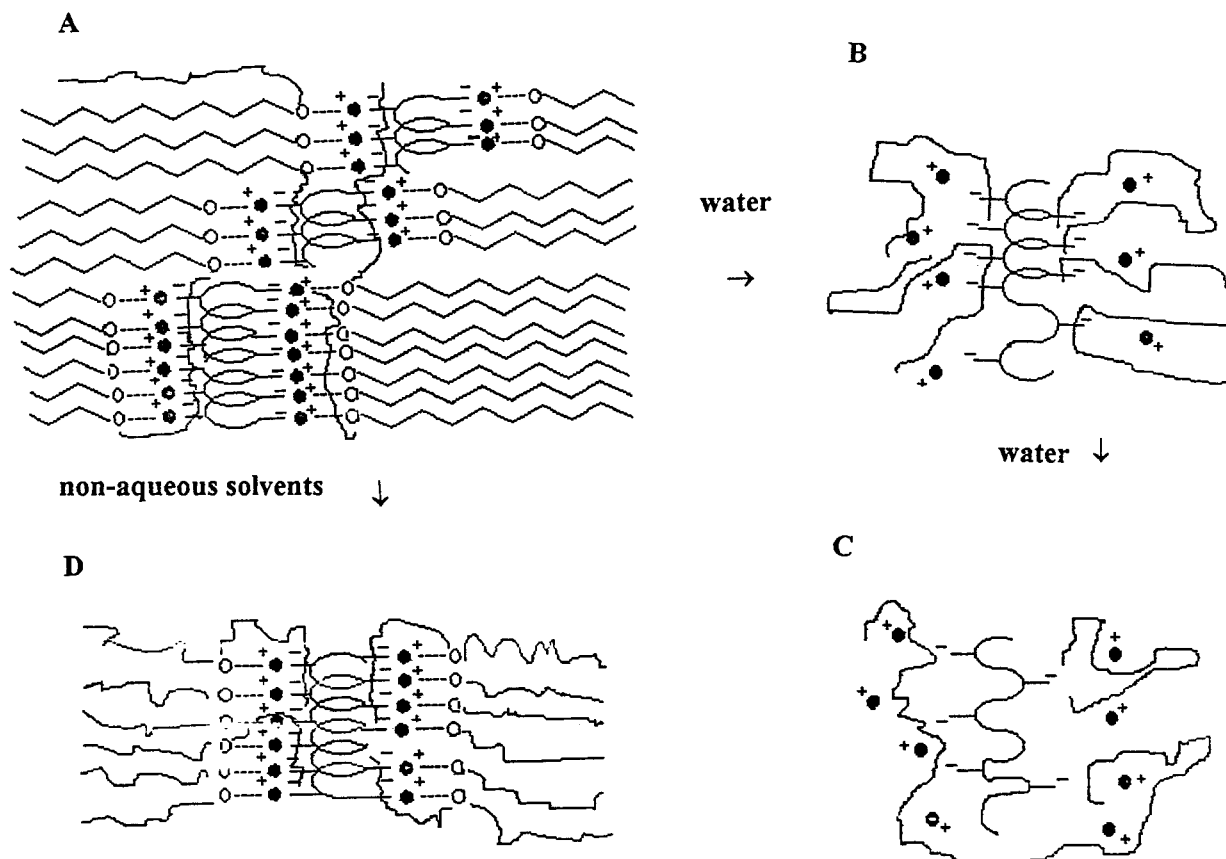


**Figure 4.** Proposed structure of PGNA 1K-PEO 600K (1:5): (A) solid-state structure; (B) in aqueous solutions (50 mg/mL); (C) in dilute aqueous solutions (1 mg/mL); (D) in dilute nonaqueous solutions.

in aqueous and nonaqueous solutions was also monitored by 2D-NOESY  $^1\text{H}$  NMR spectra using experimental condition I. Dilution of the samples in  $\text{D}_2\text{O}$  gradually weakened the correlation between methylene protons of PEO and  $\gamma$  protons of the PGNA. At a concentration of 0.6 mg/mL no correlation was observed, suggesting that at such concentrations the PEO and the PGNA are sufficiently separated for interactions to take place. This also suggests that the interactions between PEO and PGNA segments in  $\text{D}_2\text{O}$  are not strong enough to hold the segments close by when the PEO segments expand to occupy the increased volume upon dilution. If only hydrophobic interactions are holding the PEO and PGNA chains close together, dilution of nonaqueous solutions should also result in weakening of the correlation between methylene protons of PEO and  $\gamma$  protons of the PGNA. However, the strong correlation between  $\gamma$  protons of PGNA and methylene protons of PEO observed by 2D-NOESY  $^1\text{H}$  NMR spectra under condition I in  $\text{CDCl}_3$ , at 1.4 mg/mL (Figure 6), indicates that other attractive forces such as ion-dipolar interaction between sodium ion and ethylene oxide units (vide supra) must be operating in nonaqueous solutions helping PGNA and PEO segments to stay in close proximity. The 2D-NOESY  $^1\text{H}$  NMR experiment of the complexes were also conducted using experimental condition II in which the shorter mixing and relaxation times would only allow the observation of interactions in a closer proximity compared to experimental condition I. Under this condition, a good correlation between PEG protons and peptide protons in an aqueous solution of a PEG block copolymer with poly(lysine) has been observed by Harada et al.<sup>5</sup> However, the PGNA 1K-PEO 600K (1:2.5 and 1:5) and PGNA 1K-PEG 2K (1:

2.5 and 1:5) in  $\text{D}_2\text{O}$  at 50 mg/mL which showed good correlation between PEO protons and PGNA protons under experimental condition I did not show any correlation between PGNA protons and PEO protons under experimental condition II. This indicates that the PEO and the PGNA segments in these complexes are separated by a larger distance compared to the distance between the ethylene oxides and the peptide protons in the PEG-poly(lysine) block copolymer. In nonaqueous solutions (in  $\text{CDCl}_3$  and benzene), a good correlation between PGNA protons and PEO protons was observed for the PGNA 1K-PEO 600K (1:5) complex under experimental condition II even at low (1.4 mg/mL) concentrations. As suggested earlier, in nonaqueous solutions other attractive forces such as ion-dipolar interactions between PGNA and PEO segments must be operating to hold the segments in close proximity (vide supra). The 2D-NOESY  $^1\text{H}$  NMR results obtained under conditions I and II suggest that attractive intermolecular interactions between PEO and PGNA segments in nonaqueous solutions are sufficient to hold PEO and PGNA segments in close proximity even in dilute solutions. Whereas by dissolving in  $\text{D}_2\text{O}$ , interactions between methylene protons of PEO and  $\gamma$  protons of the PGNA weakened significantly and are completely absent at low concentrations (0.6 mg/mL). The concentration dependency of the "PGNA  $\gamma$  protons-PEO protons" interaction in  $\text{D}_2\text{O}$  may be explained in terms of a hydrophobic interaction. Hydrophobic interactions are usually reversible, and reattachment of the segments may not be possible if large distances due to dilution separate them. However, when molecular weight of PGNA was increased to 45K in a PGNA 45K-PEO 600K (1:5) complex, some weak correlations between

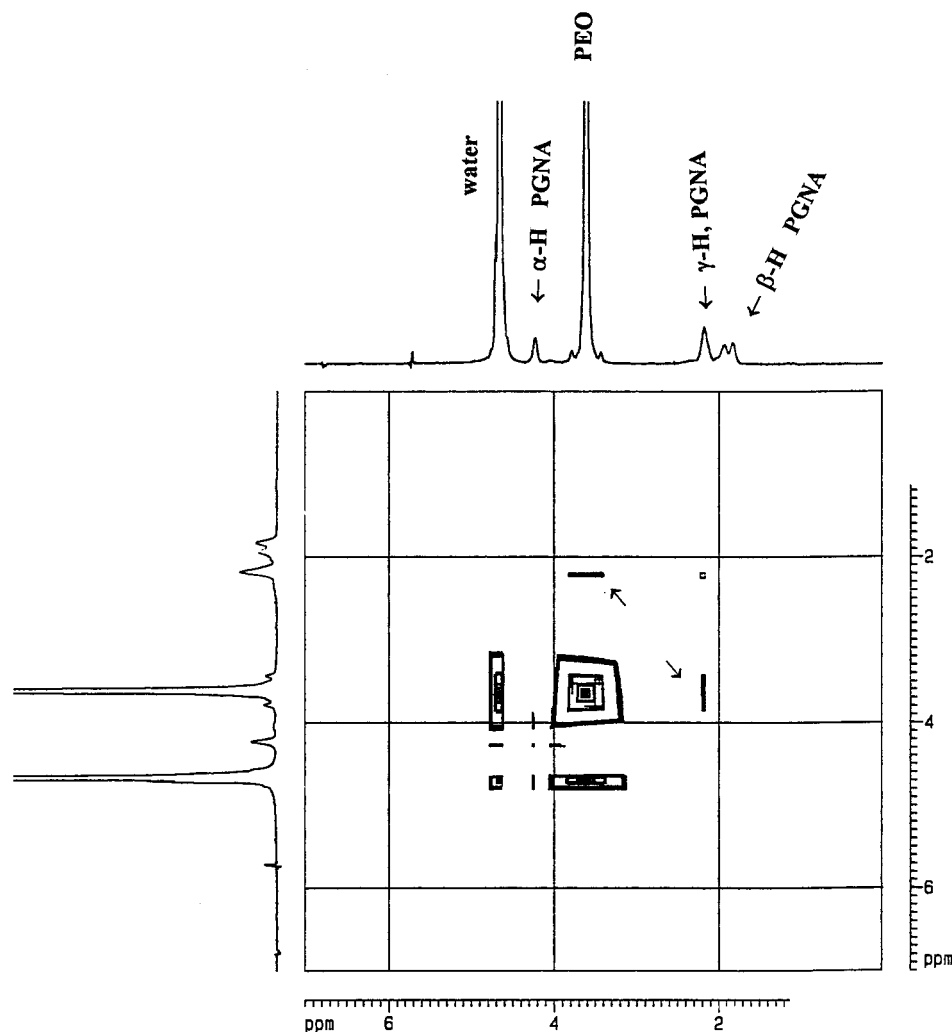


**Figure 5.** 2D-NOESY  $^1\text{H}$  NMR spectrum of PGNA 1K-PEO 600K (1:2.5) complex acquired using experimental condition I in  $\text{D}_2\text{O}$  at 50 mg/mL.

PGNA  $\gamma$  protons and PEO protons were observed even under experimental condition II in 1 mg/mL  $\text{D}_2\text{O}$  solutions. This may be explained in terms of the low probability of simultaneous detachment of every hydrophobic interaction site in the complex with PGNA of 45K. The PGNA 45K molecule has nearly 50 times more glutamate side groups carrying hydrophobic  $\gamma$  sites compared to PGNA 1K, and one PGNA 45K molecule is nearly 50 times more likely to form "PGNA  $\gamma$  site-PEO methylene group" hydrophobic attachments with a single large PEO chain such as PEO 600K. Separation of the PGNA 45K molecule from the PEO 600K molecule requires simultaneous detachment of all the "PGNA  $\gamma$  site-PEO methylene group" hydrophobic attachments. The probability of simultaneous detachment of every "PGNA (45K)  $\gamma$  site-PEO methylene group" hydrophobic site is small compared to the case of PGNA 1K, and therefore, some "PGNA  $\gamma$  site-PEO methylene group" hydrophobic interactions in the PGNA 45K-PEO 600K complex were present even in very dilute  $\text{D}_2\text{O}$  solutions. Observation of weak correlation between PGNA  $\gamma$  protons and PEO protons in dilute aqueous solution of PGNA 45K-PEO 600K complex also supports the suggestion that the nature of the interaction observed at the "PGNA  $\gamma$  protons-PEO protons" sites is reversible and presumably hydrophobic.

The ion-dipolar interactions of PEO with sodium ions of PGNA were monitored by  $^{23}\text{Na}$  NMR.  $^{23}\text{Na}$  NMR

spectra showed identical chemical shift (0.9 ppm) and identical line width (13 Hz) for both PGNA 1K and PGNA 1K-PEO 600K (1:5) in  $\text{D}_2\text{O}$ , indicating that free (solvated) sodium ion prevails in  $\text{D}_2\text{O}$  solutions in both cases. However, no signal was observed for the PGNA 1K-PEO 600K (1:5) in benzene even at a much higher number of accumulations (32 scans for the sample in  $\text{D}_2\text{O}$  and 8800 scans for the sample in benzene), indicating that the complexed form of the sodium ion has a long relaxation time as reported by Cabane<sup>7</sup> and failed to accumulate an FID during scans. No  $^{23}\text{Na}$  NMR signal was observed for the same complex in  $\text{CDCl}_3$ , indicating that sodium ions prevail 100% as complexed form in nonaqueous solutions and the complexed form appears to produce no NMR signal with 5 s delay time in single pulse acquisition. The ratio of free to complexed sodium ions in  $\text{D}_2\text{O}$  was estimated by a simple quantitative  $^{23}\text{Na}$  NMR method involving measurement of the signal intensity for a known amount of PGNA 1K-PEO 600K (1:5) in 1 mL of  $\text{D}_2\text{O}$  and estimating the amount of sodium ions by comparing the signal intensity of a standard PGNA 1K via spectral subtraction to yield a blank line. Results showed that approximately 94% of the  $\text{Na}^+$ -PEO in the complex were dissociated by dissolving in  $\text{D}_2\text{O}$  to form free (solvated) sodium ions. The  $^{23}\text{Na}$  NMR and 2D-NOESY  $^1\text{H}$  NMR results of the complexes collectively suggest that in nonaqueous solutions sodium ions of PGNA are

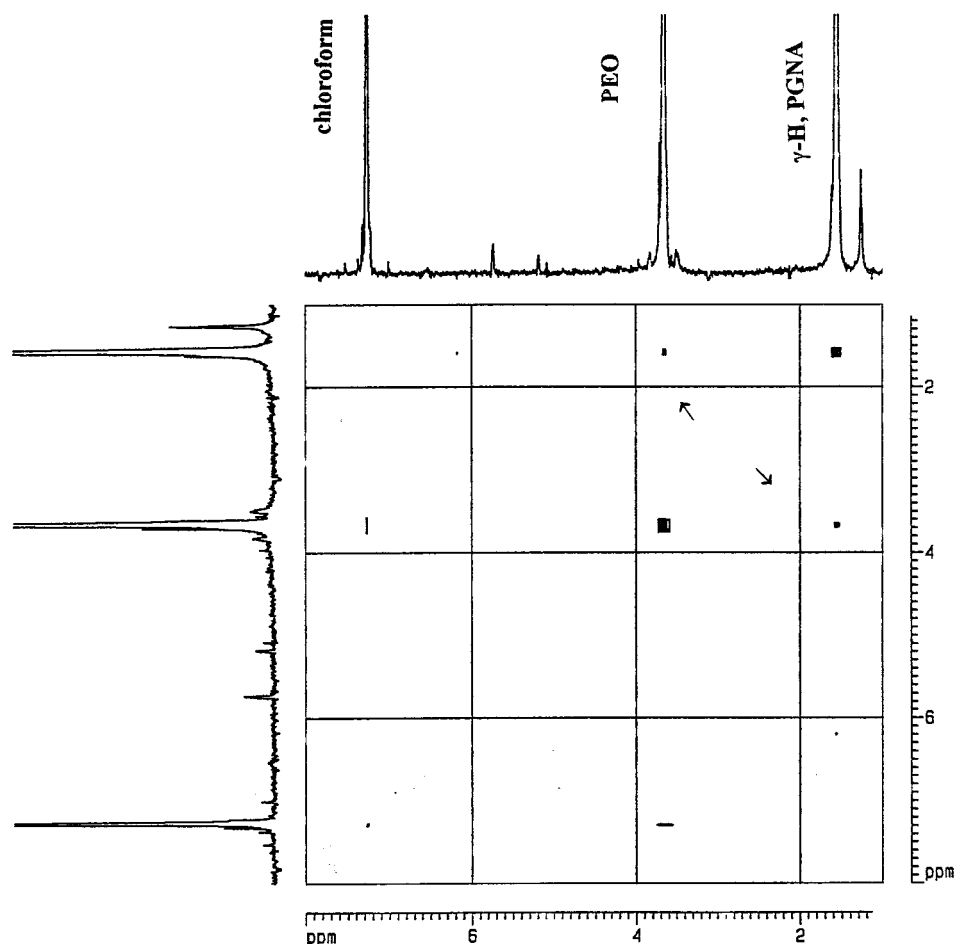


**Figure 6.** 2D-NOESY  $^1\text{H}$  NMR spectrum of PGNA 1K-PEO 600K (1:2.5) complex acquired using experimental condition I in  $\text{CDCl}_3$  at 1.4 mg/mL.

completely complexed with PEO through ion-dipole interactions. Meanwhile, the hydrophobic carbon segment of PGNA (i.e.,  $\gamma$  carbon) interacted strongly with the hydrophobic methylene segment of PEO and stayed in close proximity even in dilute solutions (Figure 4D). However by dissolving the complexes in water, nearly all of the complexed form of sodium ions were converted to free (solvated) sodium ions, and the hydrophobic interaction between PEO and PGNA was weakened significantly and completely diminished in very dilute solutions (Figure 4B,C). The hydrophobic interaction between PGNA and PEO was reversible and concentration dependent and can be increased to a certain extent by increasing the molecular weight of PGNA (to 45 000), thus allowing a higher number of points of hydrophobic interactions per poly(ethylene oxide) chain.

Combining spectral, thermal, and wide-angle X-ray data of the PGNA 1K-PEO 600K (1:5) macromolecular complex in the solid state, a probable structure of the complex is shown in Figure 4A. The proposed solid-state structure consists of a helical PGNA core; PEO crystalline segments, near the helical core, having near planar zigzag conformations; glutamate and ethylene oxide segments interacting through ion-dipolar interactions; and  $\beta$  and  $\gamma$  carbons of PGNA side groups interacting with PEO segments through hydrophobic interactions. The structure of the complex in poor nonaqueous solvents (e.g.,  $\text{CDCl}_3$ ) may be postulated as an aggregate of a molecular complex (Figure 4D) consisting of the following components: a helical PGNA core, solvated PEO segments, glutamate and ethylene oxide segments

interacting through ion-dipolar interactions, and  $\beta$  and  $\gamma$  carbons of PGNA side groups interacting with PEO segments through hydrophobic interactions. The aggregate may contain two or more complexed molecules presumably with stacked PGNA helices. The clear transparent solutions obtained using good solvents (e.g., benzene) should contain nonaggregated complexes with compositions similar to the complexes in the poor nonaqueous solvents. The structure of the complex in concentrated aqueous solutions most likely is a molecular aggregate (Figure 4B) consisting of the following components: a helical or random PGNA molecule, solvated PEO segments, and  $\beta$  and  $\gamma$  carbons of PGNA side groups interacting with PEO segments through hydrophobic interactions. The latter interaction diminishes completely in dilute aqueous solutions when the PGNA molecular weight was 1K.

## Conclusions

Solution blending of PGNA and PEO in aqueous methanol solutions followed by evaporation of the solvents leads to formation of macromolecular complexes. Properties of the complexes were dependent on both the complex stoichiometry and the molecular weights of the components. PGNA molecular weight of 1K and a stoichiometry of the PGNA:PEO of 1:5 were prerequisites for the solubility in good organic solvents. DSC, CD, and X-ray diffraction data suggest that in the solid-state both the PGNA and the PEO molecular structure were altered by complex formation. Structure of the resulting macromolecular complex may be de-



scribed as a molecular composite with the following components: a helical PGNA core, PEO crystalline segments having near planar zigzag conformations, glutamate and ethylene oxide segments interacting through ion–dipolar interactions, and  $\beta$  and  $\gamma$  carbons of PGNA side groups interacting with PEO segments through hydrophobic interactions (Figure 4).  $^{23}\text{Na}$  and 2D-NOESY  $^1\text{H}$  NMR data of the complexes in nonaqueous solvents showed that both ion–dipole and hydrophobic interactions are present even in very dilute solutions. Complete solvation (nonaggregated) of the complexes forming transparent clear dilute solutions took place in good nonaqueous solvents. The PEO segments were in close proximity in such solutions to interact strongly with the methylene side groups of PGNA presumably through hydrophobic interactions. The situation is slightly different in poor nonaqueous solvents. Both ion–dipole and hydrophobic were present in poor nonaqueous solutions, and incomplete solvation left some of the macromolecular complexes as aggregates. In aqueous solutions, the ion–dipolar interaction was completely destroyed, and the number of PGNA–PEO contact points interacting through hydrophobic interactions was reduced significantly and diminished in dilute solutions. The hydrophobic interactions between methylene carbons of PEO and  $\beta$  and  $\gamma$  carbons of PGNA side groups in dilute aqueous solutions were reversible, and reattachment in dilute solutions was possible only when molecular weight of PGNA is sufficiently large (45K).

**Acknowledgment.** Support of this work by RCM Grant 5G12RR030602 and NIH GM 08247 is gratefully acknowledged. We thank Professor Johannes Smid for valuable discussions during this study.

## References and Notes

- (1) Golander, C.-G.; Herron, J. N.; Lim, K.; Claesson, P.; Stenius, P.; Andrade, J. D. In *Poly(ethylene Glycol) Chemistry: Biotechnical and Biomedical Applications*; Harris, J. M., Ed.; Plenum Press: New York, 1992; p 221 and references therein.
- (2) Iza, M.; Stoianovici, G.; Viora, L.; Grossiord, J. L.; Couarraze, G. *J. Controlled Release* **1998**, *52*, 41.

- (3) Jeong, Y.-H.; Cheon, J.-B.; Kim, S.-H.; Nah, J.-W.; Lee, Y.-M.; Sung, Y.-K.; Akaike, T.; Cho, C.-S. *J. Controlled Release* **1998**, *51*, 169.
- (4) Gombotz, W. R.; Pettit, D. K. *Bioconjugate Chem.* **1995**, *6*, 332 and references therein.
- (5) Harada, A.; Sandrine, C.; Kataoka, K. *Macromolecules* **1996**, *29*, 6183.
- (6) Shin, G. I.; Kim, S. Y.; Lee, Y. M.; Cho, C. S.; Sung, Y. K. *J. Controlled Release* **1998**, *51*, 1.
- (7) Cabane, B. *J. Phys. Chem.* **1977**, *81*, 1639.
- (8) Point, J.-S.; Damman, P. *Macromol. Chem. Macromol. Symp.* **1990**, *39*, 301.
- (9) Dosiere, M. *Macromol. Symp.* **1997**, *114*, 51.
- (10) Point, J. J.; Damman, P. *Macromolecules* **1991**, *24*, 2019.
- (11) Li, J.; Pratt, L. M.; Khan, I. M. *J. Polym. Sci., Polym. Chem.* **1995**, *33*, 1657.
- (12) Li, J.; Khan, I. M. *Macromolecules* **1993**, *26*, 4544.
- (13) Block, H. *Poly( $\gamma$ -benzyl-L-glutamate) and Other Glutamic Acid Containing Polymers*; Gordon Breach: New York, 1983.
- (14) Ponomarenko, E. A.; Waddon, A. J.; Bakeev, K. N.; Tirrell, D. A.; MacKnight, W. J. *Macromolecules* **1996**, *29*, 4340.
- (15) Ponomarenko, E. A.; Waddon, A. J.; Tirrell, D. A.; MacKnight, W. J. *Langmuir* **1996**, *12*, 2169.
- (16) Ponomarenko, E. A.; Tirrell, D. A.; MacKnight, W. J. *Macromolecules* **1998**, *31*, 1584.
- (17) Detellier, C.; Laszlo, P. *Helv. Chim. Acta* **1976**, *59*, 1346.
- (18) Erlich, R. H.; Greenberg, M. S.; Popov, A. I. *Spectrochim. Acta* **1973**, *29A*, 543.
- (19) Gray, G. A. In *2-Dimensional NMR Spectroscopy Applications for Chemists and Biochemists*; Croasman, W. R., Carlson, R. M. K., Eds.; VCH Publishers: New York, 1987; p 58.
- (20) Seki, M.; Morishima, Y.; Kamachi, M. *Macromolecules* **1992**, *25*, 6540.
- (21) Bakeev, K. N.; Yang, M. S.; MacKnight, W. J.; Zezin, A. B.; Kabanov, V. A. *Macromolecules* **1994**, *27*, 300.
- (22) Bakeev, K. N.; Yang, M. S.; Zezin, A. B.; Kabanov, V. A. *Dokl. Akad. Nauk* **1993**, *332*, 450.
- (23) Kabanov, A. V.; Sergeev, V. G.; Foster, M.; Kasaikin, V. A.; Levashov, A. V.; Kabanov, V. A. *Macromolecules* **1995**, *28*, 3657.
- (24) Xia, D. W.; Soltz, D.; Smid, J. *Solid State Ionics* **1984**, *14*, 221.
- (25) Blout, E. R. In *Optical Rotatory Dispersion and Circular Dichroism in Organic Chemistry*; Snatzke, G., Ed.; Heyden & Son Ltd.: London, 1967; p 260.
- (26) Konig, J. L.; Frushour, B. *Biopolymers* **1972**, *11*, 1871.
- (27) Fasman, G. D.; Itoh, K.; Liu, C. S.; Lord, R. C. *Biopolymers* **1978**, *17*, 1729.
- (28) Tadokoro, H.; Chatani, Y.; Yoshihara, T.; Tahara, S.; Murahashi, S. *Macromol. Chem.* **1964**, *73*, 109.
- (29) Takahashi, Y.; Sumita, I.; Tadokoro, H. *J. Polym. Sci., Polym. Phys.* **1973**, *11*, 2113.

MA9817525